

Experimental Investigation and Multi-objective Optimization of the CNC Milling Process Parameters for Al7075 Alloys Using Taguchi-GRA and WASPAS Techniques

Randhir Kumar*, Sharifuddin Mondal

Department of Mechanical Engineering, National Institute of Technology, Patna Ashok Rajpath, Patna-800005, Bihar, India

Received 16 Jun 2025

Accepted 1 Feb 2026

Abstract

One of the key challenges in advanced machining is addressed in this paper by determining the optimal process parameters that meet both producer and customer requirements. Estimating the surface condition of a workpiece during milling remains a complex task, particularly in aerospace and automotive applications. Efficient and cost-effective CNC milling is crucial. Implementing multi-optimization approaches is essential to achieving the desired outcomes. This study systematically examines and optimizes material removal rate (MRR) and surface roughness (SR) during the milling of aluminum 7075 (Al7075). Al7075 alloys are ideal for end milling due to their excellent electrical performance, low density, high strength, stiffness, and wear resistance. The process parameters considered in this study include tool diameter, cutting speed, feed rate, and cutting depth, with a focus on their effects on MRR and SR. One way to find the minimum number of experiments needed is to use a Taguchi L9 orthogonal array. Grey Relational Analysis (GRA) and Weighted Aggregate Sum Product Assessment (WASPAS) are very efficient multi-objective approaches used to optimize milling parameters, enhancing MRR and reducing SR. The depth of cut is the most significant milling parameter influencing both MRR and SR. Optimal experimental results show an MRR of 236.39 mm³/min, 2.17 times higher than the average, and a minimum SR of 0.212 μm, 0.76 times lower than the average value.

© 2026 Jordan Journal of Mechanical and Industrial Engineering. All rights reserved

Keywords: Al7075; Milling process parameters; material removal rate; surface roughness; multi-objective optimisation.

1. Introduction

In today's market, industrial sectors prioritize high production at low costs. Manufacturing process emphasizes batch production of diverse items, utilizing aluminum, which is abundantly available in Earth's crust and widely alloyed across major sectors [1,2]. Aluminum (Al) alloys are favored for their affordability, stiffness, fatigue resistance, high specific strength, and high-temperature tolerance. The 7000 series, primarily alloyed with zinc, provides superior strength and lightness over many steels, enhanced by copper and magnesium additions [3]. Al7075 finds extensive use in automotive, defense, and aerospace industries due to its high strength and corrosion resistance, attracting growing researcher interest [4]. Al7075 undergoes rigorous machining for automotive, defense, and aerospace components, requiring optimized parameters to minimize tool wear, ensure better surface quality and accuracy, boost productivity, and reduce environmental impact [5,6,7]. Industries use conventional machining like turning, drilling, milling, and grinding for Al7075 components. Milling excels for slots, gears, and complex shapes with high speeds, precision, and flexibility [8].

Additional processes for quality or near-net shapes raise producer costs. Competitive industries prioritize productivity gains to ensure quality while minimizing machining expenses [7, 9]. Machining processes require careful optimization of input parameters to enhance productivity and satisfy customer needs. Engineers struggle to select optimal parameters amid many options and conflicting responses [10]. Machine learning (ML) integrated CNC milling simulations automatically optimize input parameters, enabling manufacturers to shorten process times while maintaining quality. Key performance metrics include surface roughness (SR) and material removal rate (MRR) [11,12]. MRR and SR are dependent on the workpiece material, tool geometry, and machining circumstances [13]. Optimizing machining requires ideal parameters, but simultaneously maximizing MRR while minimizing SR remains challenging due to their complex interactions [14]. Statistical methods like fuzzy logic, neural networks, Taguchi, factorial design, genetic algorithms, and response surface methodology optimize machining parameters [15]. Taguchi method offers economical prediction and optimization using minimum number of experiments.

* Corresponding author e-mail: randhirk.ph21.me@nitp.ac.in.

In the milling operation on Al7075-T6, Chen et al. [16] examined the various kinds of milling forces and their variation. Their study focused on the differences in forces within the plough zone and shear zone. Wirtz et al. [17] studied different techniques to choose the ideal milling process parameters for achieving optimal process stability and minimal energy consumption. With the help of ANN, Xie et al. [18] suggested a multi-objective feed rate optimization technique to improve efficiency and the stability of the machining operation. Ma et al. [19] developed virtual machining-based parameter optimization technique for multiple end milling, generating tool paths and maximizing feed rates. Pittalà and Linguanotto [20] investigated the machinability of Al7075-T6 using solid carbide end mills. Bayat and Amini [21] worked on distortion investigation in Al 7075-T6 axial ultrasonic aided milling. Ali et al. [22] experimented on vibration-assisted helical milling operation of Al7075 alloy using analytical modeling of cutting force. Dubey et al. [23] utilised the Box-Behnken technique for modeling and optimization of machining parameters in CNC end milling operations. Jayakumar and Rahman [24] studied the behavior of the end milling process on MRR and hardness variation in Al7075. Elly and Yang [25] did an experimental investigation on feed optimization for milling Al7075 using the teaching learning based optimization (TLBO) method and force modeling. Mongan et al. [26] used an ensemble neural network for optimizing a CNC milling process. Hameed et al. [27] took a multi-objective Swarm Algorithm (MSA) and neural network (NN) based modeling for optimization of CNC milling operations. Sequeira et al. [28] investigated the machining of Al7075 utilizing the Taguchi technique. Dogrusadik [29] studied cutting parameters and internal thread mill diameter effects on Al7075-T6 cutting temperature. Musavi et al. [30] evaluated tool wear and SR during the development of a micro-textured cutting tool for aluminum alloy 7075-T6 machining. Wydrzyński et al. [31] investigated the impact of unbalanced tools on surface finish in Al7075-T6 machining. Bhirud et al. [32] optimized cutting parameters for Al7075 alloys in milling using multi-objective optimization with response surface methodology and desirability approach. Patel et al. [33] optimized surface quality and thrust force in drilling Al7075 alloys using CRITIC and meta-heuristic algorithms. Singh et al. [34] optimized turning parameters for Al7075 alloys to minimize tool wear and surface roughness.

This study focuses on the optimization of milling process parameters for high-strength Al7075 alloys, using key machining parameters identified from existing literature, including speed, feed, tool diameter, and depth of cut. To minimize the number of experiments, the Taguchi method that minimizes experiments as a robust single-objective technique for either MRR or SR, building on prior predictions of MRR and SR is applied. While existing CNC milling studies offer valuable insights into forces, stability, feed optimization, tool wear, and temperatures, significant gaps persist in multi-objective optimization for simultaneous MRR maximization and SR minimization, both response effectively. To address this, the study incorporates an advanced soft-computing approach, utilizing an experimental design to assess the effects of process parameters on both MRR and SR during Al7075 CNC milling operation. The findings refined optimal process parameters through ANOVA, Taguchi-gray relational analysis, and WASPAS. This approach is both straightforward and less complex, offering a more efficient

means of optimization for improved production and surface quality in industrial applications.

2. Experimental Details

This research is conducted using a CNC milling machine (Chandra model 2015) manufactured by BFW, India. Specimen preparation for mechanical testing adheres to ASTM standards, CNC machining used to produce samples conforming to E8 dimensions. The trials are conducted using Taguchi's L9 orthogonal array design. The Al7075 alloy workpiece used for the experiments had a width of 50 mm and a length of 160 mm. Figure 1 shows the specimens of Al7075 alloys before and after machining. It was securely clamped onto the machine's worktable. The weighing machine (Venus Electronics Digital Weighing Scale, Ace Incorporation, INDIA) whose measurement range is 1gm to 10kg was used in the experiment. It measures the weight of materials both before and after machining. Surface roughness measurements were taken using a pocket-sized Marsurf surface roughness tester, ideal for quick, on-site inspection. The surface roughness measuring instruments are shown in Figure 2.

2.1. Al7075 material

Al7075-T6 alloys is a matrix material frequently used in aerospace and defense applications, such as shafts, gears, valve components, and missile parts. It is heat-treatable and commonly used in structural applications. Al7075 alloys offer high strength, stiffness, and acceptable fatigue behavior. It also has remarkable resistance to corrosion, creep, and wear [35]. A rectangular bar of 60mm breadth and 165 mm length is used as the Al7075 workpiece for the milling process. The material for experimentation is sourced from M/s. Bharat Aerospace Metals, Mumbai. The Al7075-T6 composition (Zn≈5.30, Mg≈2.15, Si≈1.50, Cu≈1.23, Na≈0.80, Cr≈0.20, Fe≈0.16, and Mn≈0.15 by weight%) is used as a base alloy material with more specifications [3]. The detailed specifications of Al7075 are shown in Table 1. The important mechanical properties of Al7075 alloys are presented in Table 2 [36].

Table 1. Detailed the specifications of Al7075 [3]

Base matrix	Thermal conductivity	Young modulus	Melting point	Elongation	Density	Poisson ratio
Al7075-T6	130 w/m-k	72GPa	480°C	11%	2.81gm/cc	0.33

Table 2. Mechanical properties of Al7075 [36]

Mechanical Properties	At cast	Heat treated (T6)
Tensile Strength (MPa)	150	360
Hardness (VHN)	98.4	181
Micro-hardness	58	61
Impact strength (J)	23	15
Yield strength (MPa)	114	451
Elongation %	10.67	8.34
Porosity %	0.5	0.5

2.2. CNC Milling Machine

A rectangular slab is made using Al7075 alloys of the dimensions 165mm x 50mm x 10mm. The experiments are carried out using a CNC milling machine. The machine's maximum travel capabilities are X=800 mm, Y=350 mm, and Z=389 mm, with an accuracy of 0.005 mm. Milling operations are performed on the Al7075 alloy using tool diameters of 8 mm, 10 mm, and 12 mm. During the milling process, operations were performed on the workpiece while considering the appropriate process parameters [32]. The Al7075 alloy material was then inserted into the jaw of the bed and tightened as shown below. The difference between the starting and end weights was taken to calculate the material removal rate (MRR) during the experiment.

2.3. Material Removal Rate and Surface Roughness

This section mainly discusses the material removal rate and surface roughness of Al7075 alloys. Enhancement of surface quality during machining operations depends on the material removal rate. Surface roughness is a key factor in machining and is used to determine machining quality. Al7075 alloy is selected for its excellent strength-to-weight ratio which fits extensive applications in aircraft

components such as fuselage frames and wing spars, military equipment, including vehicles and weapons, and high-performance racing car parts.

2.3.1. Material Removal Rate (MRR)

To conduct the MRR experiments, various input parameters are selected, including tool diameter, spindle speed, feed rate, and depth of cut, during milling operation. The selection of the four input parameters and three levels is based on the findings from pilot experiments and the operator's knowledge. Before each experiment, the upper and lower surfaces of the workpiece are cleaned to remove any dust. This eliminates unwanted particles, ensuring efficient machining of the Al7075 alloy material. The MRR can be measured using equation (1) for this experiment [37]. The weights of Al7075 alloys are recorded before and after experiments using a digital weighing machine that has a weight measurement range from 1g to 10kg.

$$\text{MRR (mm}^3/\text{min)} = \frac{1000 \times \text{WL}}{T_e \times \rho_c} \quad (1)$$

Where W_a = Weight loss after machining (g), W_b = Weight loss before machining (g), WL = Weight loss of workpiece ($W_b - W_a$), ρ_c = Density of Al7075 material (2.81 g/cm³), T_e = Time taken by one sample during experiment (min).

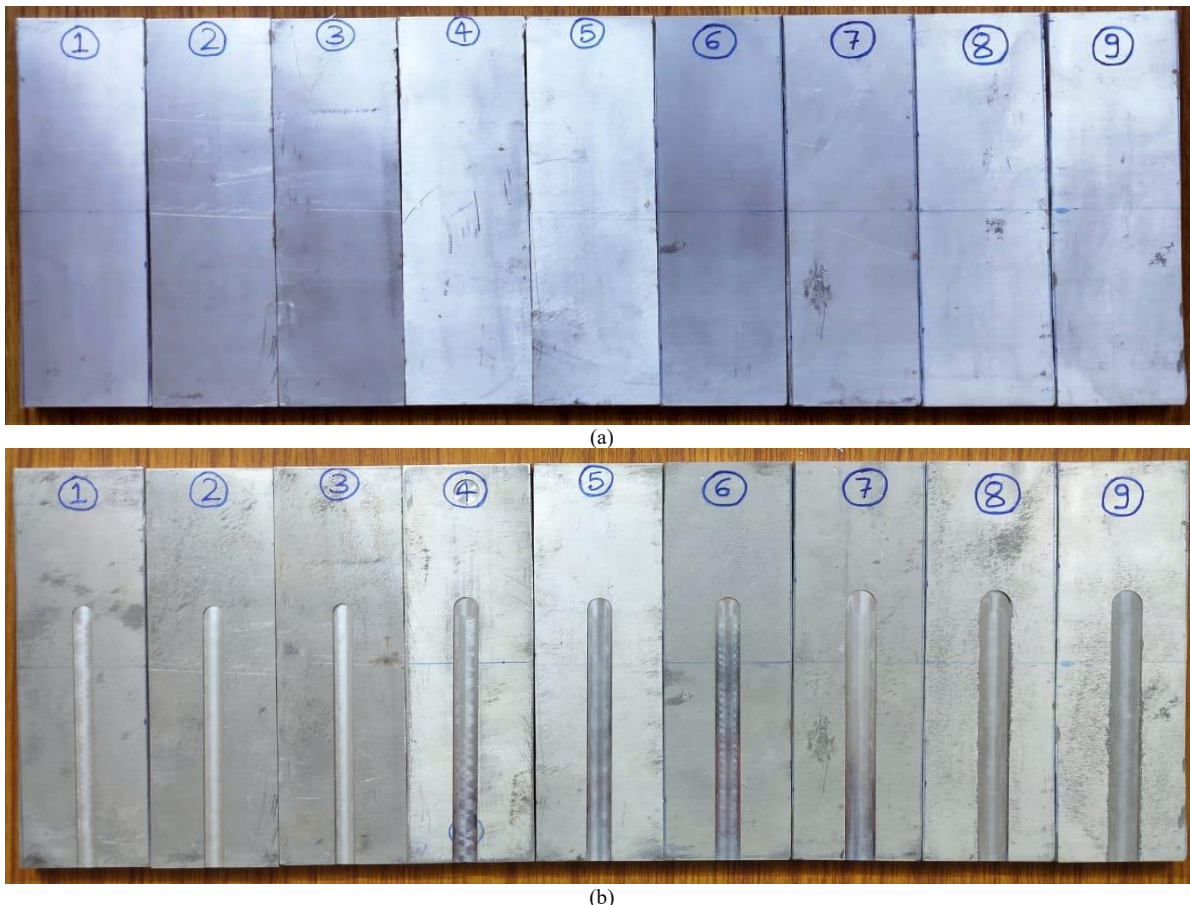


Figure 1. Al7075-T6 alloys workpieces a) before machining and b) after machining

2.3.2. Surface Roughness (SR)

A Marsurf surface roughness tester is used to determine the SR of the product specimen. This device accurately determined the roughness values. Roughness factors, such as Ra, were measured at three separate locations. Ra is the arithmetic mean of the roughness measurement. Figure 2 shows the surface roughness measurement taken from a milling sample. Similarly, all 9 sample measurements are listed in Table 4.

3. Design of Experiment (DOE)

This study employs the Taguchi optimization technique to minimize the number of experiments required. It supports in efficiently achieving the optimal condition. The Taguchi technique [1, 3, 7, 28] has been widely used to determine the best process parameter settings for the machining processes. To optimize the milling process, four input factors are considered at three different levels: tool diameter (mm), spindle speed (rpm), depth of cut (mm), and feed rate (mm/rev). The experiments are designed using the Taguchi DOE methodology. The L9 orthogonal array is selected for the experimental setup. Minitab-19 software is used to perform the design process. Table 3 shows the control factors and levels for the experimental setup of Al7075 alloys. These combinations produced a total of nine experimental parameter settings. Table 4 summarizes the milling operations along with their corresponding levels. The dependent parameter, MRR, is measured using equation (1). SR is determined by using the roughness tester packet instruments.

Table 3. Control factors for the experimental setup of Al7075 alloys

Parameters	Level (1)	Level (2)	Level (3)
Tool diameter (TD)	8	10	12
Spindle speed (SS)	500	1000	1500
Feed rate (FR)	10	20	30
Depth of cut (DOC)	0.25	0.5	1.0

The experiments follow the Taguchi L9 orthogonal array design. This is designed based on the data presented in Table 4. This approach helps us to reduce cost and save time. The Taguchi approach is to convert output response into signal-to-noise (S/N) ratios. The responses are commonly used to determine the S/N ratio of three types: smaller-the-better, larger-the-better, and nominal-the-better. This study aims to achieve a material removal rate (higher-the-better) and lower surface roughness (smaller-the-better) and make the criterion the most appropriate for optimizing these factors.

The equation used for obtaining the S/N ratio for the larger-the-better responses,

$$S/N = (-10) \log_{10} \left(\frac{1}{n} \sum_{i=1}^n \frac{1}{y_i^2} \right) \quad (2)$$

For calculating the S/N ratio for the smaller-the-better responses,

$$S/N = (-10) \log_{10} \left(\frac{1}{n} \sum_{i=1}^n y_i^2 \right) \quad (3)$$

Where, 'y_i' refers to the experimental response of the ith experiment, 'i' represents the specific experiment number, and 'n' indicates the overall number of experiments conducted. The optimal conditions are identified by analyzing the average S/N ratios at each level. A mathematical model is then developed using the general regression approach. The experimental framework and procedural design of this study is shown in Figure 3.



Figure 2. Surface roughness measuring experimental setup

Table 4. Experimental result based on L9 orthogonal array for milling operation

Sample no	Tool diameter (mm)	Spindle speed (rpm)	Feed rate (mm/rev)	Depth of cut (mm)	MRR (mm ³ /min)	SR (µm)	S/N (MRR)	S/N (SR)
1	8	500	10	0.25	19.23	0.285	25.6796	10.9031
2	8	1000	20	0.50	77.22	0.408	37.7546	7.7868
3	8	1500	30	1.00	233.24	0.534	47.3561	5.4492
4	10	500	20	1.00	190.48	0.201	45.5970	13.9361
5	10	1000	30	0.25	71.43	0.436	37.0776	7.2103
6	10	1500	10	0.50	47.62	0.260	33.5558	11.7005
7	12	500	30	0.50	170.94	0.154	44.6569	16.2496
8	12	1000	10	1.00	113.21	0.377	41.0777	8.4732
9	12	1500	20	0.25	56.60	0.109	35.0563	19.2515

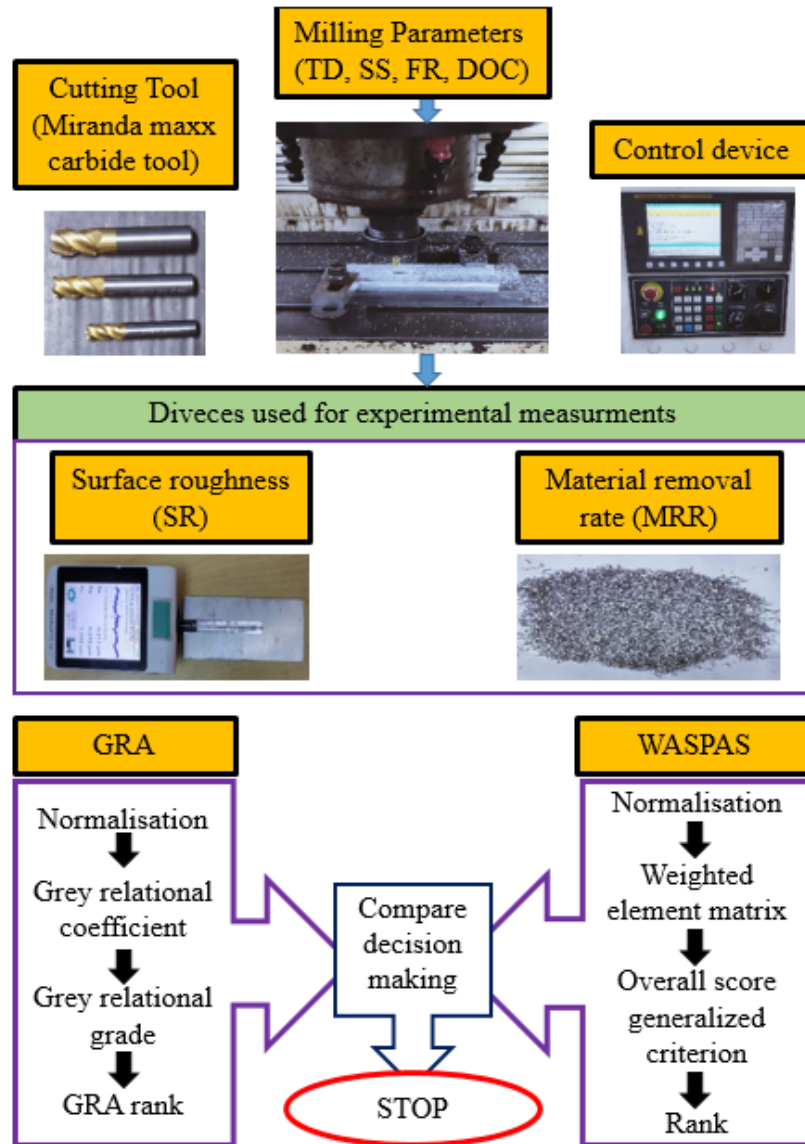


Figure 3. Methodology of the current work architecture

4. Multi-Objective Optimization Techniques

Multi-response optimization is particularly valuable in manufacturing because it helps finding solutions that strike a balance between conflicting goals. In machining, for instance, increasing MRR and improving surface finish are often opposing objectives, which make it necessary to use multi-objective optimization to satisfy all objectives simultaneously.

Over the years, different multi-response optimization techniques have been developed and applied to improve the milling process of mechanical components, adjusting cutting conditions to boost competitiveness [38]. This study uses two of these methods, GRA and WASPAS, to find the best outcomes. Both methods primarily focus on analyzing the signal-to-noise ratio of MRR and SR.

4.1. Grey Relational Analysis (GRA) method

The Taguchi techniques combined with GRA can be used to find out the optimal process parameters for milling of Al7075 alloys. This approach helps maximizing the

material removal rate while minimizing surface roughness[39,40]. This approach has become a highly effective technique for solving multi-objective optimization issues. GRA converts a multi-characteristic optimization problem into a single-objective problem. This transformation enables the identification of the best parameter settings.

Step I: Normalizing the measured responses is the first stage in the GRA process. The two kinds of quality criteria that are commonly used for normalization in GRA are larger-the-better and smaller-the-better. This research requires both maximizing and minimizing responses. Therefore, normalization is performed using both the larger-the-better and smaller-the-better characteristics.

In the GRA approach[41,42], the following steps are used to find the optimal results as given below:

The pre-processing result, $y_i^*(k)$, the higher the better, normalized mode for MRR can be expressed as:

$$y_i^*(k) = (x_i^0(k) - \min x_i^0(k)) / (\max x_i^0(k) - \min x_i^0(k)) \quad (4)$$

For lower the better, normalization mode for SR can be expressed as:

$$y_i^*(k) = (\max x_i^0(k) - x_i^0(k)) / (\max x_i^0(k) - \min x_i^0(k)) \quad (5)$$

Where 'i' is the experiment number and 'k' is the quality characteristics, $\max x_i^0(k)$ is the highest value among $x_i^0(k)$, $\min x_i^0(k)$ is the lowest value among $x_i^0(k)$, and $x_i^0(k)$ is the experiment's responses.

Step II: The next equation for the GRA is to find the grey relational co-efficient (GRC) can be expressed as:

$$\xi_i(k) = (\Delta_{\min} + \psi\Delta_{\max}) / (\Delta_{0i}(k) + \psi\Delta_{\max}) \quad (6)$$

Where, $\Delta_{0i}(k) = |\max x_i^0(k) - x_i^0(k)|$, Δ_{\max} is the maximum value for $\Delta_{0i}(k)$, and Δ_{\min} is the minimum value for $\Delta_{0i}(k)$. ψ is the distinctive co-efficient that lies between $0 \leq \psi \leq 1$ (ψ is generally taken as 0.5 by default).

Step III: The final step in GRA is to calculate the grey relational grade (GRG). This is done by averaging the sum of the grey relational coefficients (GRC) using the following equation. The GRG is expressed as:

$$\gamma_i = \frac{1}{n} \sum_{k=1}^n \xi_i(k) \quad (7)$$

Where γ_i lies between the values of 0 to 1, and the experiment number is denoted by n.

The optimal parameter setting has a higher grey relational grade (GRG). Parameters with greater GRG values are closer to the optimum solution. The GRG values of the parameters are used to rank them.

4.2 Weighted Aggregate Sum Product Assessment (WASPAS) method

Weighted Aggregate Sum Product Assessment (WASPAS) is a recent optimization technique. Both single-response and multiple-response optimization problems can be resolved using it. It is perhaps the simplest technique for solving a multi-criteria decision-making (MCDM) problem [38, 43, 44]. Like other MCDM approaches, its implementation begins with the creation of the initial decision matrix. The next step is to establish the relevant weight vector. This technique is initially given by Zavadskas, who used the weighted sum model (WSM) and weight product model (WPM). In this research, the WASPAS techniques are conducted using the signal-to-noise ratio of Taguchi method. To find the optimal parameters, the steps of the WASPAS techniques [45,46] can be expressed as:

Step I: The first decision matrix is defined based on the S/N ratio matrix as shown in Table 4. The weight vectors are expressed as follows.

$$[W_1, W_2, \dots, W_n] = W_j \text{ Where, } \sum_{j=1}^n W_j = 1$$

There are several methods for a weight measurement approach, where W_j is a weight attributed to the jth criterion. MRR and SR are two responses with equal weightage are assigned for this research.

Step II: The decision matrix is normalized using two equations, and the resulting normalized values are presented in WASPAS rank Table.

$$\text{Maximisation } \bar{X}_{ij} = \frac{x_{ij}}{\max_i x_{ij}} \quad (8)$$

$$\text{Minimisation } \bar{X}_{ij} = \frac{\min_i x_{ij}}{x_{ij}} \quad (9)$$

Step III: The WASPAS is obtained by relating with the WSM and WPM approach. The weight sum model (WSM)

and weight product model (WPM) are used to determine the overall relative relevance of the i^{th} alternative, which are represented by equations (10) and (11), respectively.

$$\text{WSM} = Q_i^{(1)} = \sum_{j=1}^n \bar{X}_{ij} * W_j \quad (10)$$

$$\text{WPM} = Q_i^{(2)} = \prod_{j=1}^n (\bar{X}_{ij})^{W_j} \quad (11)$$

According to the WSM and WPM, Q_1 and Q_2 are determined. Based on the j^{th} criterion, the significance of the i^{th} alternative is found out. Here, W_j is the weight.

Step IV: The additive and multiplicative approaches are used in the joint generalized criterion for weight aggregation. The following equation is used to calculate WASPAS as given below

$$\text{WASPAS} = Q_i = \psi * Q_i^{(1)} + (1 - \psi) * Q_i^{(2)} \quad (12)$$

$$= \psi * \sum_{j=1}^n \bar{X}_{ij} W_j + (1 - \psi) * \prod_{j=1}^n (\bar{X}_{ij})^{W_j} \quad (13)$$

Here, the symbol ψ lies between $0 \leq \psi \leq 1$ (By default, ψ is used as 0.5). Higher values correspond to a higher ranking by the researchers. For the greatest Q_i value, the top rank is assigned.

5. Results and Discussion

The experimental results are analysed using Minitab 16, a statistical analysis software. To find out how TD (tool diameter), SS (spindle speed), FR (feed rate), and DOC (depth of cut) affect the responses, ANOVA examines the outputs, here SR and MRR.

5.1. Taguchi Analysis

5.1.1.1. Analysis of the signal-to-noise ratio (S/N ratio) for MRR

The signal-to-noise (S/N) ratio has been used to evaluate how control parameters like TD, SS, FR, and DOC affect the material removal rate. This analysis helps evaluating their influence on performance. The MRR is graphically shown in Figure 4 with the mean S/N ratio. In Figure 5 provides a graphic representation of the effect of means on MRR. The results show that when the cutter diameter changes from 8 to 10 mm, the thickness of the chips produced increases as well. Faster feed rates are frequently made possible by the 12mm diameter cutting tool, which raises the rate of material removal. But it can also make chip evacuation more difficult. This could make the machining process less effective [47]. As cutting speed increases from 500 to 1000 rpm, cutting force decreases due to thermal softening. This softening alters the shear angle, reducing the required plastic deformation. However, when the speed increases further from 1000 to 1500 rpm, the cutting force may rise again. This is primarily due to increase in strain and strain rate [48]. Increasing the feed rate and depth of cut improves the MRR of milling of Al7075 alloy materials [34]. According to results analyzed, the parameters combination that produces the highest MRR for the range of parameters examined is TD = 12mm, SS = 500 rpm, FR = 30 mm/rev, and DOC = 1mm.

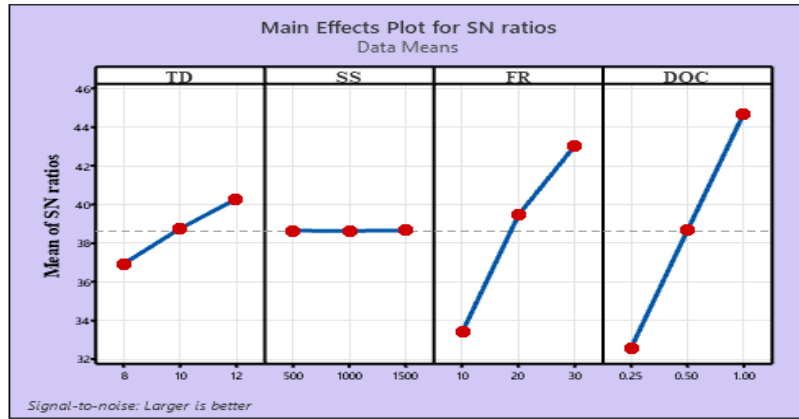


Figure 4. MRR Vs S/N ratio

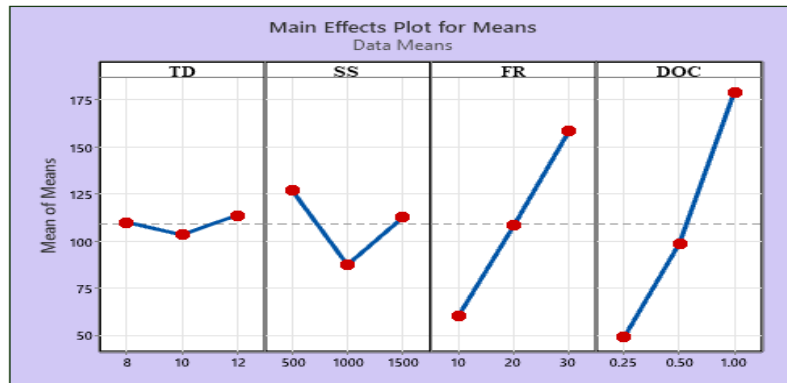


Figure 5. MRR variation with TD, SS, FR, and DOC

The response graph's greater S/N value showed the best MRR. The graph shows that the maximum MRR is achieved with a factor combination of 12mm TD, 500rpm SS, 30 mm/rev FR, and 1mm DOC. This combination optimizes material removal efficiency. The maximum MRR of the developed combination is obtained when TD, FR, and DOC are at the highest level and SS is at the lowest level. DOC is the most important element out of all of them, according to Table 5 and Table 6 (S/N ratio response). FR and TD come after it, and SS is less important.

5.1.2. Analysis of the S/N ratio (signal-to-noise ratio) for SR

For the milling process to yield a high-quality, low-energy, and cost-effective product, a minimum degree of surface roughness must be maintained. The "lower the better" quality criteria are utilized to determine the S/N ratio because the aim is to minimize surface roughness. Plotting the mean S/N ratio values facilitates the analysis of the impact of each factor level on the outputs. Figure 6 shows how each parameter affects the outcome. The factor level with the highest mean S/N ratio indicates the optimal condition. The ideal conditions maximize the performance for that specific element. In Figure 7 presents the main effect plot for mean illustrating the effects of TD, SS, FR, and DOC.

Figure 6 shows that larger size of TD gives a better quality SR with respect to the smaller size TD. Furthermore, the SR is lowered because the concentrated pressure is reduced and the forming forces are distributed over a larger region [49]. Raising the cutting speed from 500 to 1000 rpm results in a noticeable decrease in surface roughness.

However, the roughness clearly rises as speed increases. At lower cutting rates, chip breakup results in a rough surface. Both chip breakage and roughness decrease with speed [50]. Higher feed and depth of cut require the removal of more material at once, which strains the tool more. For the cutting operation, this also means that more energy is needed. As a result, the greater cutting force degrades the quality of the machined surface [51]. Based on the previously provided information, the optimum condition for SR results in the following conditions for enhanced surface quality: 12mm TD, 1000 SS, 20 FR, and 0.25mm DOC. TD is the most important element out of all of them, according to Table 7 and Table 8 (S/N ratio response). SS and FR come after it, and DOC is less important.

Table 5. Response for MRR S/N ratios: Larger is better: Signal-to-Noise ratios response

Level	TD	SS	FR	DOC
1	36.93	38.64	33.44	32.60
2	38.74	38.64	39.47	38.66
3	40.26	38.66	43.03	44.68
Delta	3.33	0.02	9.59	12.07
Rank	3	4	2	1

Table 6. Response for MRR S/N ratios: Larger is better: Response for means

Level	TD	SS	FR	DOC
1	109.90	126.88	60.02	49.09
2	103.18	87.29	108.10	98.59
3	113.58	112.49	158.54	178.98
Delta	10.41	39.60	98.52	129.89
Rank	4	3	2	1

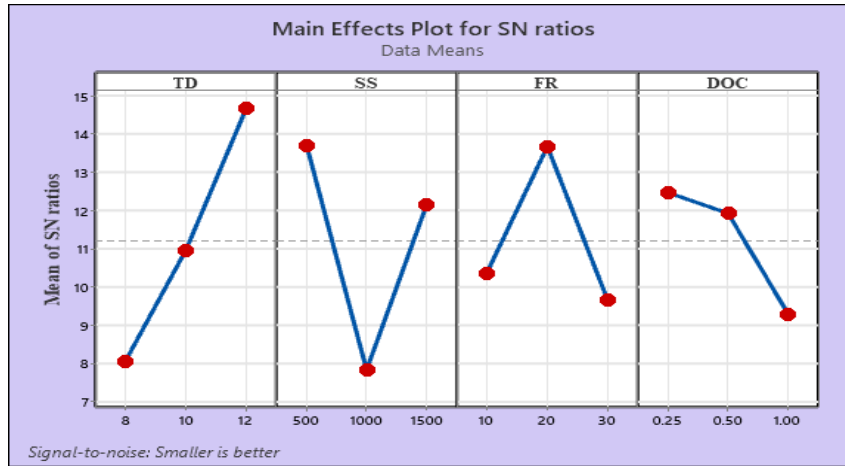


Figure 6. Main effect plot for SR

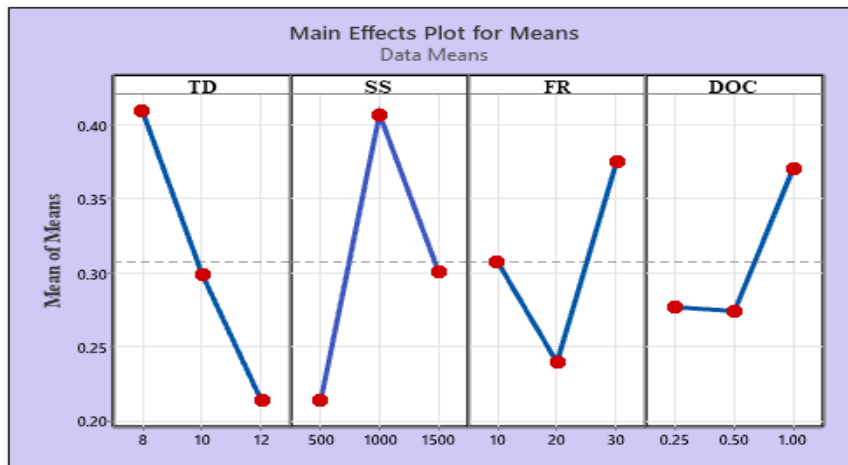


Figure 7. SR variation with TD, SS, FR, and DOC

Table 7. Response for SRS/N ratios: Smaller the better: Signal-to-Noise ratios response

Level	TD	SS	FR	DOC
1	8.046	13.696	10.359	12.455
2	10.949	7.823	13.658	11.912
3	14.658	12.134	9.636	9.286
Delta	6.612	5.873	4.022	3.169
Rank	1	2	3	4

Table 8. Response for SR S/N ratios: Smaller the better: Response for means

Level	TD	SS	FR	DOC
1	0.4090	0.2133	0.3073	0.2767
2	0.2990	0.4070	0.2393	0.2740
3	0.2133	0.3010	0.3747	0.3707
Delta	0.1957	0.1937	0.1353	0.0967
Rank	1	2	3	4

5.1.3. ANOVA for MRR and SR

ANOVA gives the percentage contribution that mainly affects the output characteristics. ANOVA results obtained for MRR and SR are shown in Table 9 and Table 10, respectively. From the ANOVA Table, it is found that MRR is significantly influenced by DOC, followed by FR, SS, and TD, respectively. The percentage contribution of each factor is 60.07%, 33.92%, 5.62%, and 0.39%, respectively. Similarly, in the case of SR, it is just the reverse of the MRR affected input parameters. It is seen that surface quality is significantly influenced by TD, SS, FR, and DOC, respectively. Each of these factors contributes

36.12%, 35.31%, 17.19%, and 11.38%, respectively. More details are shown below:

Table 9. ANOVA of MRR

Parameters	Degree of freedom	Sum of squares	Mean squares	% contribution
TD	2	167.0	83.5	0.39
SS	2	2410.2	1205.1	5.62
FR	2	14561.1	7280.5	33.92
DOC	2	25783.8	12891.9	60.07
Total	8	42922.1		

Table 10. ANOVA of SR

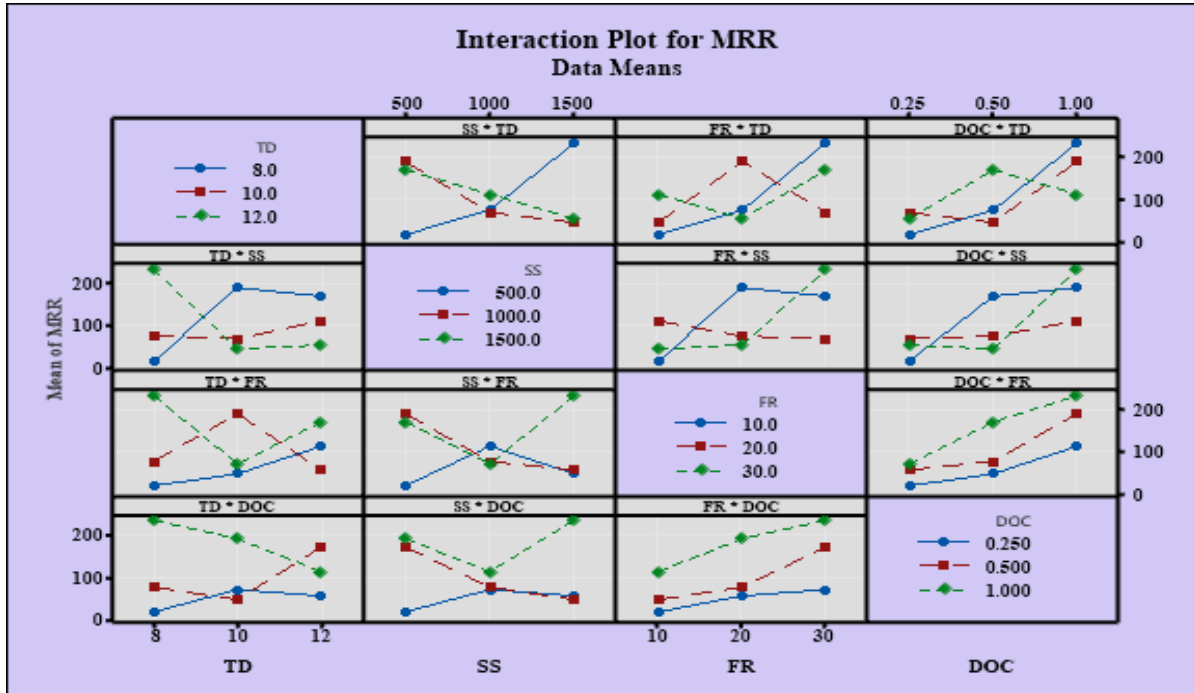
Parameters	Degree of freedom	Sum of squares	Mean squares	% contribution
TD	2	0.05772	0.028862	36.12
SS	2	0.05643	0.028214	35.31
FR	2	0.02747	0.013736	17.19
DOC	2	0.01819	0.009094	11.38
Total	8	0.15981		

5.1.4. Interaction Plot

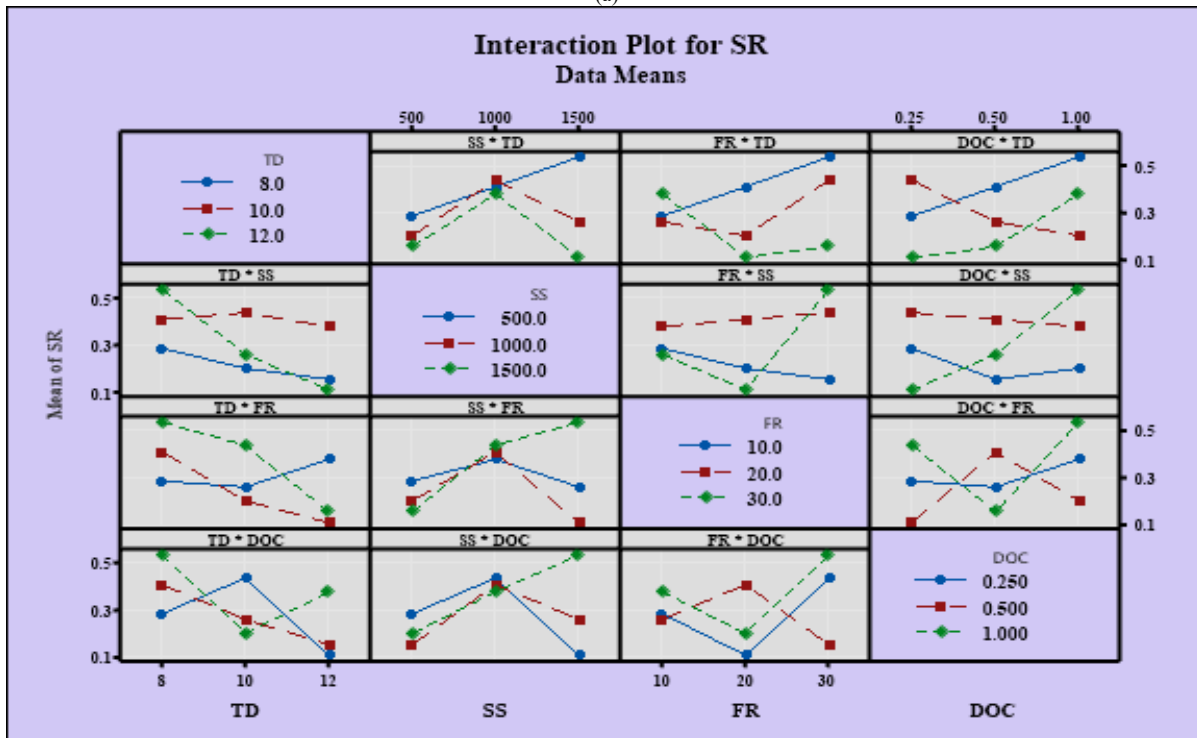
The effect of the CNC milling input parameters on the response variable is shown in Figure 8. The graph shows that with a minimum tool diameter (TD) of 8 mm, both the MRR and SR are higher. These values are greater compared to the other two TD levels. It is also observed that for a minimum tool diameter (TD) of 8 mm, the material removal rate (MRR) and surface roughness (SR) are higher compared to the other two TD values. The both responses MRR with SR show an upward trend due to increasing the feed rate (FR)

and depth of cut (DOC). The best surface finish is achieved at a TD of 12 mm. In addition, for higher spindle speed (SS) of 1500 rpm, MRR increases slightly with TD, but shows a more rapid increase with FR and DOC. Conversely, SR shows the opposite trend. When a higher FR is used, MRR initially slows down as TD increases from 8 mm to 10 mm and SS increases from 500 rpm to 1000 rpm, after which the MRR increases. Both DOC and FR tend to increase MRR. For achieving a good surface finish, a TD of 10 mm is

preferable for higher FR of 30 mm. Increasing DOC to 1 mm improves MRR with FR, but decreases with TD. The interaction between DOC and SS initially reduces MRR, but eventually leads to an increase. The best surface finish is observed with a TD of 12 mm and a lower DOC of 0.25 mm. For higher DOC values, a lower SS of 500 rpm and a medium FR of 20 mm/rev provide the best results. The more details of the interaction effect of the input factor on the output responses are shown in Figure 8.



(a)



(b)

Figure 8. Interaction plot between input factor and response variables: (a) MRR (b) SR

5.1.5. Normal Probability Curve

A 95% confidence interval generates probability plots that illustrate and interpret the experimental results. Plots make it clear that the majority of the data are close to one another around the center fitted line, confirming the experimental data distribution's normality assumption. A statistical technique called the Anderson–Darling (AD) test [52,53], which looks for outliers, provides additional support for the normalcy assumption. If the p-value is greater than 0.05, the null hypothesis of the AD test supports the assumption of normality. However, if the p-value is less than 0.05, the alternative hypothesis rejects the normality claim of the null hypothesis. As Figure 9 shows, all of the responses have p-values greater than 0.05, the data are normally distributed, and should be used for further optimization and investigation.

5.2. Grey Rational Analysis (GRA)

For the output response, the machining performance is given in Table 4 and is normalized initially using equations (4) and (5). The grey relational coefficient (GRC) value for each output is calculated by using equation (6). Finally GRG value is obtained by assigning equal weightage for all outputs in our research. Among the L9 experiments, the parameter combination with the highest GRG is regarded as rank 1 as shown in Table 11. It is observed that experiments 3 gives the highest GRG value, thus its rank is 1. Therefore, it is considered the best in this study. Among the L9 Taguchi experiments conducted, Experiment 3 exhibits the optimal process parameter combination for multi-objective optimization.

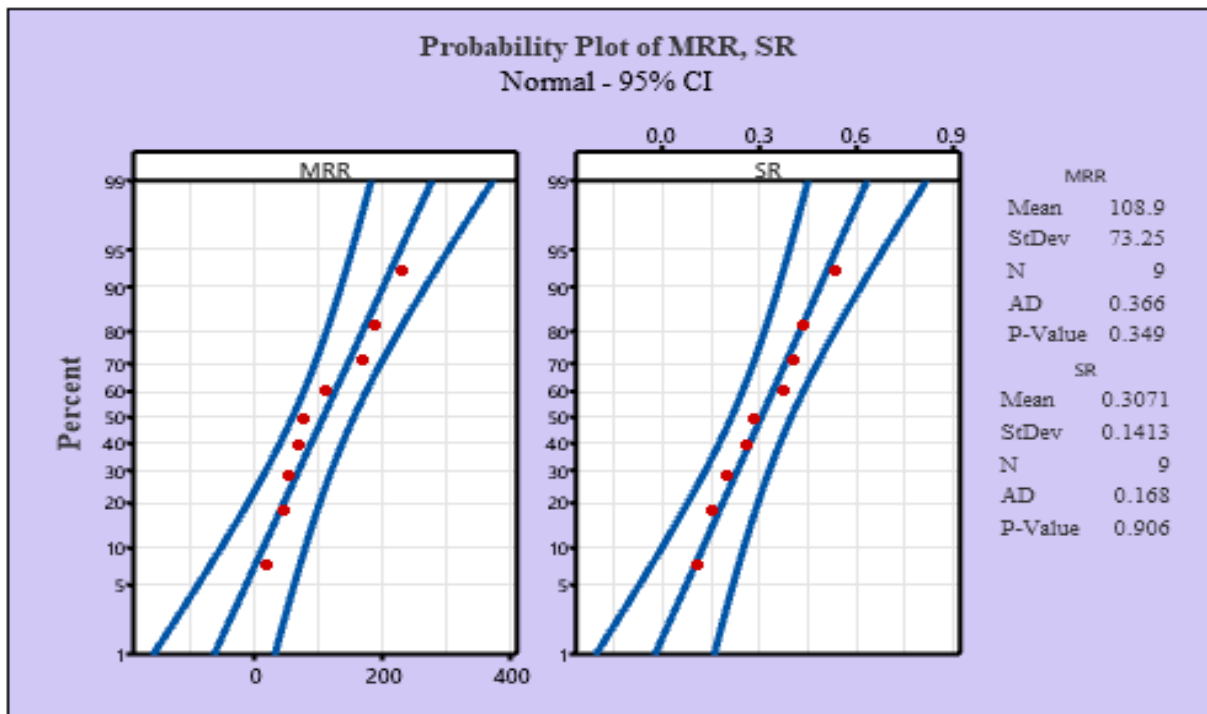


Figure 9. Normal probability curve for the response variable.

Table 11. Calculated normalized, GRC, GRG, and rank for L9 experiments

S No	Normalization		GRC		GRG	Rank
	MRR	SR	MRR	SR		
1	0	0.60	0.33	0.56	0.444	8
2	0.56	0.83	0.53	0.75	0.639	5
3	1	1	1	1	1	1
4	0.92	0.39	0.86	0.45	0.656	3
5	0.53	0.87	0.52	0.79	0.655	4
6	0.36	0.55	0.44	0.53	0.482	7
7	0.88	0.22	0.81	0.39	0.599	6
8	0.71	0.78	0.63	0.69	0.664	2
9	0.43	0	0.47	0.33	0.400	9

Table 12. Means Table for GRG

Level	TD	SS	FR	DOC
1	0.6943	0.5663	0.5300	0.4997
2	0.5977	0.6527	0.5650	0.5733
3	0.5543	0.6273	0.7513	0.7733
Delta	0.1400	0.0863	0.2213	0.2737
Rank	3	4	2	1

According to Table 12 for mean GRG, the following parameters, which are highlighted in bold, are ideal for the highest GRG: a 1000 rpm speed, 30 mm/min feed rate, 8mm tool diameter, and 1mm depth of cut. The corresponding data is presented in Figure 10. The GRG ANOVA results show that every factor considered has a significant impact, with p-values below 0.05 at a 95% confidence level. Based on the sequential sum of squares used to calculate the contribution percentage, DOC has the maximum influence on GRG at 48.54%. It is followed by FR at 34.26%, TD at 12.43%, and SS at 4.77%.

5.3. Weighted Aggregate Sum Product Assessment (WASPAS)

The experimental observations shown in Table 4 for the experimental output are normalized first by using equations

(8) and (9). The WASPAS is obtained by the WSM and WPM methods using equations (10) and (11). The WASPAS value for each output is calculated by using equation (12). Finally, the WASPAS value is obtained by allowing equal weightage to all of the responses. The rank is assigned on the basis of the Q_i value, as shown in Table 13. The parameter combination with the highest Q_i is considered rank 1 among the L9 experiments conducted. In all 9 experimental Q_i values, experiment 3 provides the maximum value. Thus, its rank is considered as 1. In this study, Experiment 3 is identified as having the best process parameter combination. It achieves optimal multi-objective optimization among the L9 experiments used.

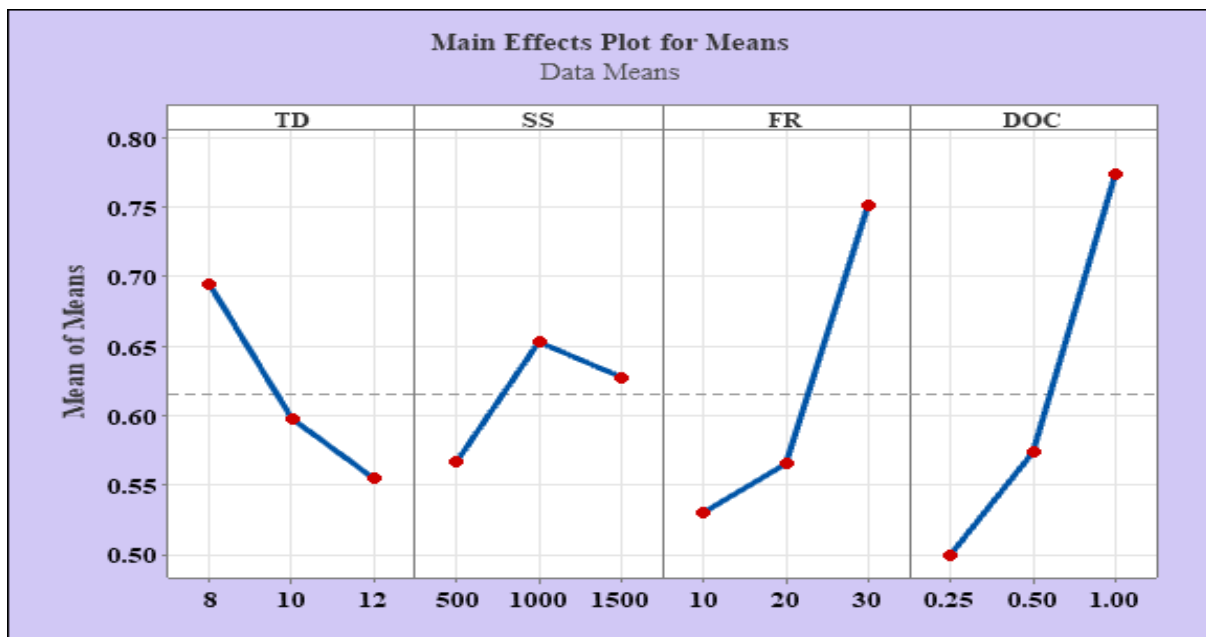


Figure 10. Main effect plot for GRG

Table 13. Results of the optimization by the WASPAS method

S. no	Normalization		Weighted valuation values			RANK
	MRR	SR	Q_1	Q_2	Q_i	
1	0.5423	0.4998	0.5210	0.5206	0.5208	8
2	0.7972	0.6998	0.7485	0.7469	0.7477	4
3	1	1	1	1	1	1
4	0.9629	0.3910	0.6769	0.6136	0.6453	5
5	0.7830	0.7558	0.7694	0.7692	0.7693	2
6	0.7086	0.4657	0.5872	0.5845	0.5808	7
7	0.9430	0.3353	0.6392	0.5623	0.6008	6
8	0.8674	0.6431	0.7553	0.7469	0.7511	3
9	0.7403	0.2831	0.5117	0.4578	0.4847	9

Table 14. Means Table for WASPAS

Level	TD	SS	FR	DOC
1	0.7562	0.5890	0.6176	0.5916
2	0.6651	0.7560	0.6259	0.6431
3	0.6122	0.6885	0.7900	0.7988
Delta	0.1440	0.1671	0.1725	0.2072
Rank	4	3	2	1

The Table 14 provides the optimum value for maximum Q_i for WASPAS techniques, i.e. 8mm TD, 1000 SS, 30 mm/min FR, and 1mm DOC, is highlighted, and Figure 11 is the corresponding graph. Every factor taken into account has a significant effect, according to the WASPAS ANOVA (p values are less than 0.05 at a 95% confidence level). The sequential sum of square values is used to calculate the contribution percentage. It shows that DOC has the highest impact on Q_i at 34.78%, followed by FR at 28.27%, SS at 21.11%, and TD at 15.85%.

5.4. Confirmation Test

To identify the optimal parameters setting, in WASPAS techniques, Q_i data and for GRA techniques, GRG data are important. The optimal parameter combination is specified by each method according to its own assessment. In the CNC milling machine, a final confirmation experiments are run on the optimal process parameters on Al7075 alloys. The observed value are shown in the Table 15 using GRA and WASPAS methods. It can be found that the result obtained by both methods are optimum MRR and SR.

6. Conclusion and Future Scope

This study focuses on optimizing a multi-response problem using the GRA and WASPAS methods, with Al7075 alloys. The main aim is to maximize MRR for increased production and minimum SR to ensure a high-quality surface finish. Although multi-criteria decision-

making methods continue to evolve, optimizing CNC milling process parameters remains complex. This experimental study on Al7075 alloys provides a valuable comparison between traditional methods and advanced soft-computing techniques like multi-objective WASPAS and GRA, where GRA and WASPAS algorithms address challenges by balancing conflicting responses through conversion of simple multi-objective optimization to single-response problem. For Al7075 alloys, optimal parameters maximize MRR while minimizing SR. Depth of cut emerges as the most influential parameter for GRG and Q_i in both GRA and WASPAS approaches, followed by FR, while SS and TD rank as the least significant factors. Taguchi optimizes MRR and SR separately, while GRA/WASPAS identifies minimum TD (8 mm), medium SS (1000 rpm), highest FR (30 mm/min), and maximum DOC (1 mm) for the highest MRR=236.39 mm³/min and lowest SR=0.232 μ m, effectively balancing both responses. Taguchi single-objective optimization yields a maximum MRR of 344.90 mm³/min (corresponding SR of 0.261 μ m) or minimum SR of 0.212 μ m (corresponding MRR of 58.82 mm³/min), but GRA/WASPAS enhances MRR 2.17 times and reduces SR 0.76 times average values. ANOVA confirms DOC (48.54%) and FR (34.26%) as dominant contributors, with SS (21.11%) and TD (15.85%) the least influential. For future work, other multi-objective techniques such as Multi-Attributive Real-Ideal Comparative Analysis (MARICA), the Combined Compromise Solution (CoCoSo) method, and weight-based approaches like the Best Worst Method (BWM) can be explored.

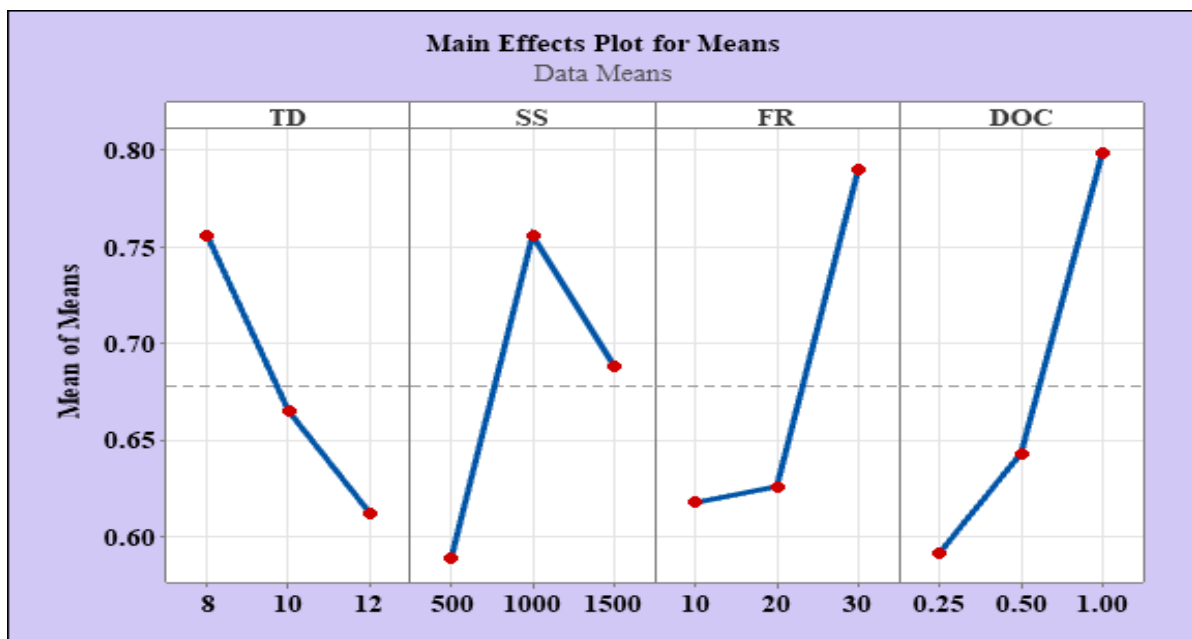


Figure 11. Main effect plot for WASPAS

Table 15. Optimum level of milling process parameters and responses

Method	TD	SS	FR	DOC	MRR(mm ³ /min)	SR(μ m)
Taguchi method (for MRR)	12	500	30	1	344.90	0.261
Taguchi method (for SR)	12	500	20	0.25	58.82	0.212
GRA	8	1000	30	1	236.39	0.232
WASPAS	8	1000	30	1	236.39	0.232

Author's contributions

The study's conception and design are contributed to by all authors. Randhir Kumar and SharifuddinMondal are responsible for preparing the materials, collecting the data, and analyzing the results. The first draft of the manuscript is written by Randhir Kumar, while SharifuddinMondal provided comments on the earlier drafts. All authors reviewed and gave their approval for the final version of the manuscript.

Acknowledgement

The authors express their sincere gratitude to the Department of Mechanical Engineering at NIT Patna for providing the necessary infrastructure to conduct this research.

Compliance with Ethical Standards

Conflict of interest: No conflicts of interest are associated with this study, as confirmed by the authors.

Funding: Funding for this research study did not provided by any specific grant from funding agencies.

Data availability statement: Since no such data was extracted from any of the study's publications, it has nothing to do with this paper. There are no human rights violations or any valid ethical or security issues because neither humans nor animals are engaged.

Reference

- [1] Akhtar, Mohammad Nishat, T. Sathish, V. Mohanavel, Asif Afzal, K. Arul, M. Ravichandran, InzarulfaihamAbd Rahim, S. S. N. Alhady, Elmi Abu Bakar, and B. Saleh. "Optimization of process parameters in CNC turning of aluminum 7075 alloy using L27 array-based Taguchi method." *Materials*, Vol. 14, No. 16, 2021, pp. 44-70. <https://doi.org/10.3390/ma14164470>
- [2] Patel, GC Manjunath, Deepak Lokare, Ganesh R. Chate, Mahesh B. Parappagoudar, R. Nikhil, and Kapil Gupta. "Analysis and optimization of surface quality while machining high strength aluminium alloy." *Measurement*, Vol. 152, 2020, pp. 1-17. <https://doi.org/10.1016/j.measurement.2019.107337>
- [3] Singh, Nikhilesh, Rm Belokar, RsWalia, and Ashish Rathee. "Parametric study of eco-friendly reinforcements on aluminium based hybrid MMC using Taguchi approach." *Advances in Materials and Processing Technologies*, Vol. 8, No. 4, 2022, pp. 4440-4451. <https://doi.org/10.1080/2374068X.2022.2077281>
- [4] Kumar, Randhir, and SharifuddinMondal. "Role of different reinforcements in aluminium 7075-based metal matrix composite—a review." *SAE International Journal of Materials and Manufacturing*, Vol. 17, No. 05-17-04-0025, 2024, pp. 355-364. <https://doi.org/10.4271/05-17-04-0025>.
- [5] Maranhão, C., J. P. Davim, and M. J. Jackson. "Physical thermomechanical behavior in machining an aluminium alloy (7075-O) using polycrystalline diamond tool." *Materials and Manufacturing Processes*, Vol. 26, No. 8, 2011, pp. 1034-1040. <https://doi.org/10.1080/10426914.2010.520794>
- [6] Makadia, Ashvin J., and J. I. Nanavati. "Optimisation of machining parameters for turning operations based on response surface methodology." *Measurement*, Vol. 46, No. 4, 2013, pp. 1521-1529. <https://doi.org/10.1016/j.measurement.2012.11.026>
- [7] Asiltürk, İlhan, and SüleymanNeşeli. "Multi response optimisation of CNC turning parameters via Taguchi method-based response surface analysis." *Measurement*, Vol. 45, No. 4, 2012, pp. 785-794. <https://doi.org/10.1016/j.measurement.2011.12.004>
- [8] Xu, Feng, Jian Jun Zhu, Xiao Jun Zang, and Xin Wu. "Rapid parameter optimization of high speed milling aluminum alloy thin-walled workpiece." *Key engineering materials*, Vol. 431, 2010, pp. 41-44. <https://doi.org/10.4028/www.scientific.net/KEM.431-432.41>
- [9] Pusavec, F., and J. Kopac. "Achieving and implementation of sustainability principles in machining processes." *Journal of Advances in Production Engineering and Management*, Vol 3, No. 4, 2009, pp. 58-69.
- [10] Kalita, Kanak, S. Madhu, M. Ramachandran, Shankar Chakraborty, and Ranjan Kumar Ghadai. "Experimental investigation and parametric optimization of a milling process using multi-criteria decision making methods: a comparative analysis." *International Journal on Interactive Design and Manufacturing (IJIDeM)*, Vol. 17, No. 1, 2023, pp. 453-467. <https://doi.org/10.1007/s12008-022-00973-3>
- [11] Masooth, P. HajaSyeddu, V. Jayakumar, and G. Bharathiraja. "Experimental investigation on surface roughness in CNC end milling process by uncoated and TiAlN coated carbide end mill under dry conditions." *Materials Today: Proceedings*, Vol. 22, 2020, pp.726-736. <https://doi.org/10.1016/j.matpr.2019.10.036>
- [12] Maher, Ibrahim, M. E. H. Eltaib, Ahmed AD Sarhan, and R. M. El-Zahry. "Investigation of the effect of machining parameters on the surface quality of machined brass (60/40) in CNC end milling—ANFIS modeling." *The International Journal of Advanced Manufacturing Technology*, Vol. 74, No. 1, 2014, pp. 531-537. <https://doi.org/10.1007/s00170-014-6016-z>
- [13] Reddy, B. Sidda, J. Suresh Kumar, and K. Vijaya Kumar Reddy. "Optimization of surface roughness in CNC end milling using response surface methodology and genetic algorithm." *International Journal of Engineering, Science and Technology*, Vol. 3, No. 8 , 2011, pp. 102-109. <https://doi.org/10.1007/s00170-014-6016-z>
- [14] Santos, Renan C., Milton Pereira, and Joao CE Ferreira. "Energy consumption in milling as a result of different machining parameters and tool paths." In *2020 IEEE Green Technologies Conference (GreenTech)*, 2020, pp. 206-211. [IEEE. 10.1109/GreenTech46478.2020.9289747](https://doi.org/10.1109/GreenTech46478.2020.9289747)
- [15] Marler, R. Timothy, and Jasbir S. Arora. "Function-transformation methods for multi-objective optimization." *Engineering Optimization*, Vol. 37, No. 6, 2005, pp. 551-570. <https://doi.org/10.1080/03052150500114289>
- [16] Chen, Yinghua, Tao Wang, and Guoqing Zhang. "Research on parameter optimization of micro-milling Al7075 based on edge-size-effect." *Micromachines*, Vol. 11, No. 2, 2020, pp. 1-15. <https://doi.org/10.3390/mi11020197>
- [17] Wirtz, Andreas, Dirk Biermann, and Petra Wiederkehr. "Design and optimization of energy-efficient milling processes using a geometric physically-based process simulation system." *Procedia CIRP*, Vol. 88, 2020, pp. 270-275. <https://doi.org/10.1016/j.procir.2020.05.047>
- [18] Xie, Jiejun, Pengyu Zhao, Pengcheng Hu, Yang Yin, Huicheng Zhou, Jihong Chen, and Jianzhong Yang. "Multi-objective feed rate optimization of three-axis rough milling based on artificial neural network." *The International Journal of Advanced Manufacturing Technology*, Vol. 114, No. 5, 2021, pp.1323-1339. <https://doi.org/10.1007/s00170-021-06902-0>
- [19] Ma, Hengyuan, Wei Liu, Xionghui Zhou, QiangNiu, and Chuipin Kong. "An effective and automatic approach for parameters optimization of complex end milling process based on virtual machining." *Journal of Intelligent Manufacturing*,

- Vol. 31, No. 4, 2020, pp. 967-984. <https://doi.org/10.1007/s10845-019-01489-6>
- [20] Pittalà, Gaetano M., and Stefano Linguanotto. "A study of machinability of Al7075-T6 with solid carbide end mills." *Procedia CIRP*, Vol. 115, 2022, pp. 148-153. <https://doi.org/10.1016/j.procir.2022.10.065>
- [21] Bayat, Masuod, and SaeidAmini. "Distortion analysis in axial ultrasonic assisted milling of Al 7075-T6." *International Journal of Lightweight Materials and Manufacture*, Vol. 7, No. 5, 2024, pp. 678-687. <https://doi.org/10.1016/j.ijlmm.2024.04.003>
- [22] Ali, Mariam Nabil, Hesham Khalil, and Hassan El-Hofy. "Analytical modeling of cutting force in vibration-assisted helical milling of Al 7075 alloy." *Journal of Manufacturing Processes*, Vol. 119, 2024, pp. 372-384. <https://doi.org/10.1016/j.jmappro.2024.03.094>
- [23] Dubey, Vineet, Prameet Vats, Harish Kumar, and Anuj Kumar Sharma. "Optimization and Modelling of Machining Parameters in End Milling Operation Using Box-Behnken Technique." In *International Conference on Mechanical and Energy Technologies*, Singapore: Springer Nature Singapore, 2023, pp. 485-495. https://doi.org/10.1007/978-981-97-2716-2_43
- [24] Jayakumar, K., and PJ Abdul Rahman. "Effect of end milling parameters on MRR and hardness variation of AA7075." *Materials Today: Proceedings*, Vol. 72, 2023, pp. 2212-2216. <https://doi.org/10.1016/j.matpr.2022.09.199>
- [25] Elly, Ogotulsaya, and Yin Yang. "Feed optimization based on force modelling and TLBO algorithm in milling Al 7075." *Journal of the Brazilian Society of Mechanical Sciences and Engineering*, Vol. 46, No. 5, 2024, pp. 1-16. <https://doi.org/10.1007/s40430-024-04839-5>
- [26] Mongan, Patrick G., Eoin P. Hinchy, Noel P. O'Dowd, Conor T. McCarthy, and Nancy Diaz-Elsayed. "An ensemble neural network for optimising a CNC milling process." *Journal of Manufacturing Systems*, Vol. 71, 2023, pp. 377-389. <https://doi.org/10.1016/j.jmsy.2023.09.012>
- [27] Hameed, Azzam S., BijanMallick, KrishnenduMondal, and S. K. Hikmat. "Neural network (NN) based modelling and Multi-objective Swarm Algorithm (MSA) optimization of CNC milling operation." *Materials Today: Proceedings*, 2023, pp. 1-9. <https://doi.org/10.1016/j.matpr.2023.03.076>
- [28] Sequeiera, Anil, D. Deepak, and H. K. Sachidananda. "Experimental study on machining of AA7075 using Taguchi method." *SN Applied Sciences* Vol. 5, No. 1, 2023, pp. 1-8. <https://doi.org/10.1007/s42452-022-05249-9>
- [29] Dogrusadik, Ahmet. "Effect of cutting conditions and thread mill diameter on cutting temperature in internal thread milling of Al7075-T6." *Sādhanā* Vol. 47, No. 3, 2022, pp. 1-7. <https://doi.org/10.1007/s12046-022-01935-x>
- [30] Musavi, Seyed Hasan, Majid Seprehkia, Behnam Davoodi, and Seyed Ali Niknam. "Performance analysis of developed micro-textured cutting tool in machining aluminum alloy 7075-T6: assessment of tool wear and surface roughness." *The International Journal of Advanced Manufacturing Technology*, Vol. 119, No. 5, 2022, pp. 3343-3362. <https://doi.org/10.1007/s00170-021-08349-9>
- [31] Wydrzyński, Dawid, ŁukaszPrzeszlowski, GrzegorzBudzik, and BartoszKamiński. "Impact of Tool Imbalance on Surface Quality in Al7075-T6 Alloy Machining." In *International Conference on Industrial Measurements in Machining*, Cham: Springer International Publishing, 2019, pp. 226-235. https://doi.org/10.1007/978-3-030-49910-5_20
- [32] Bhirud, N. L., A. S. Dube, Amit S. Patil, and Kiran Suresh Bhole. "Multi-objective optimization of cutting parameters and helix angle for temperature rise and surface roughness using response surface methodology and desirability approach for Al 7075." *International Journal on Interactive Design and Manufacturing (IJIDeM)*, Vol. 18, No. 10, 2024, pp. 7095-7114. <https://doi.org/10.1007/s12008-023-01285-w>
- [33] Patel, GC Manjunath, and Jagadish. "Experimental modeling and optimization of surface quality and thrust forces in drilling of high-strength Al 7075 alloy: CRITIC and meta-heuristic algorithms." *Journal of the Brazilian Society of Mechanical Sciences and Engineering*, Vol. 43, No. 5, 2021, pp. 1-21. <https://doi.org/10.1007/s40430-021-02928-3>
- [34] Singh, Jasjeevan, Simranpreet Singh Gill, and Amit Mahajan. "Experimental investigation and optimizing of turning parameters for machining of al7075-t6 aerospace alloy for reducing the tool wear and surface roughness." *Journal of Materials Engineering and Performance*, Vol. 33, No. 17, 2024, pp. 8745-8756. <https://doi.org/10.1007/s11665-023-08584-z>
- [35] Singh, Ranjeet Kumar, and Ramesh Chandra Singh. "Evaluation of the mechanical and microstructural properties of an Al7075/B4C/Gr FGM plate fabricated using a stir casting process." *Journal of Mechanical Science and Technology*, Vol. 38, No. 10, 2024, pp. 5389-5398. <https://doi.org/10.1007/s12206-024-0913-3>
- [36] Kumar, Randhir, and SharifuddinMondal. "Effects of inorganic reinforcements on microstructural, mechanical, tribological, and machining characteristics of stir cast Al7075 composite: A review." *Proceedings of the Institution of Mechanical Engineers, Part C: Journal of Mechanical Engineering Science*, Vol. 239, No. 12, 2025, pp. 4687-4725. <https://doi.org/10.1177/09544062251324344>
- [37] Aruri, Devaraju, MurahariKolli, SatyanarayanaKosaraju, and G. Sai Kumar. "RSM-TOPSIS multi optimization of EDM factors for rotary stir casting hybrid (Al7075/B4C/Gr) composites." *International Journal on Interactive Design and Manufacturing (IJIDeM)*, 2022, pp.1-16. <https://doi.org/10.1007/s12008-022-00893-2>
- [38] Safi, Khaoula, Mohamed AthmaneYallese, Salim Belhadi, Tarek Mabrouki, and AissalLaouissi. "Tool wear, 3D surface topography, and comparative analysis of GRA, MOORA, DEAR, and WASPAS optimization techniques in turning of cold work tool steel." *The International Journal of Advanced Manufacturing Technology*, Vol. 121, No. 1, 2022, pp. 701-721. <https://doi.org/10.1007/s00170-022-09326-6>
- [39] Bhuvanesh Kumar, M., P. Sathiyaa, and R. Parameshwaran. "Parameters optimization for end milling of Al7075-ZrO₂-C metal matrix composites using GRA and ANOVA." *Transactions of the Indian Institute of Metals*, Vol. 73, No. 11, 2020, pp. 2931-2946. <https://doi.org/10.1007/s12666-020-02089-2>
- [40] Mohanta, Dillip Kumar, BidyadharSahoo, and ArdhenduMouliMohanty. "Optimization of process parameter in Al7075 turning using grey relational, desirability function and metaheuristics." *Materials and Manufacturing Processes*, Vol. 38, No. 12, 2023, 1615-1625. <https://doi.org/10.1080/10426914.2023.2165671>
- [41] Kumar, Dhiraj, and SharifuddinMondal. "Multi-attribute optimization of edm process parameters of Al-2050 alloy using taguchi based topsis and GRA with different rotating tools." *International Journal of Modern Manufacturing Technologies (IJMMT)*, Vol. 13, No. 1, 2021, pp. 84-95.
- [42] Gopal, P. M., and K. Soorya Prakash. "Minimization of cutting force, temperature and surface roughness through GRA, TOPSIS and Taguchi techniques in end milling of Mg hybrid MMC." *Measurement*, Vol. 116, 2018, pp. 178-192. <https://doi.org/10.1016/j.measurement.2017.11.011>
- [43] Akgün, Hasret, EceYapıcı, AysunÖzkan, ZerrinGünkaya, and MüfideBanar. "A combined multi-criteria decision-making approach for the selection of carbon-based nanomaterials in phase change materials." *Journal of Energy Storage*, Vol. 60, 2023, pp. 1-12. <https://doi.org/10.1016/j.est.2023.106619>
- [44] Kumar Ghadai, Ranjan, Shankar Chakraborty, and Kanak Kalita. "On solving parametric optimization problem of an end milling process for machining of Al 1070 using MCDM techniques: a comparative analysis." *Advances in materials*

- and processing technologies, Vol. 10, No. 3, 2024, pp. 2421-2443. <https://doi.org/10.1080/2374068X.2023.2216398>
- [45] Mallikarjuna, P., P. Prasanna, P. Sivaiah, and V. Chengal Reddy. "MQL turning processing of EN24 alloy steel material with novel textured tools." *Materials and Manufacturing Processes*, Vol. 40, No. 13, 2025, pp. 1713-1724. <https://doi.org/10.1080/10426914.2025.2549261>
- [46] Arif, Rashique, SharifuddinMondal, and NimaiPada Mandal. "WASPAS based Taguchi approach to reduce the energy consumption of a typical office building." *Proceedings of the Institution of Mechanical Engineers, Part C: Journal of Mechanical Engineering Science*, Vol. 239, No. 14, 2025, pp. 5709-5725. <https://doi.org/10.1177/09544062251327546>
- [47] Daniyan, Ilesanmi, KhumbulaniMpofu, Festus Fameso, Isaac Tlhabadira, and Solomon Phokoby. "Computer-aided modelling and experimental evaluation of the pocket milling operation for alloy tool steel (AISI D3)." *The International Journal of Advanced Manufacturing Technology*, Vol. 122, No. 11, 2022, pp. 4453-4466. <https://doi.org/10.1007/s00170-022-09979-3>
- [48] Shankar, Sachindra, Kush P. Mehta, SomnathChattopadhyaya, and Pedro Vilaça. "Dissimilar friction stir welding of Al to non-Al metallic materials: An overview." *Materials chemistry and physics*, Vol. 288, 2022, pp. 1-25. <https://doi.org/10.1016/j.matchemphys.2022.126371>
- [49] Bishnoi, Pawan, and Pankaj Chandna. "Optimizing the SPIF parameters for enhancing microhardness and surface quality in Inconel 625 superalloy components." *Journal of Alloys and Compounds*, Vol. 997, 2024, pp. 174839. <https://doi.org/10.1016/j.jallcom.2024.174839>
- [50] Korkmaz, Mehmet Erdi, Munish Kumar Gupta, ErdalÇelik, NimelSworna Ross, and Mustafa Günay. "A sustainable cooling/lubrication method focusing on energy consumption and other machining characteristics in high-speed turning of aluminum alloy." *Sustainable Materials and Technologies*, Vol. 40, 2024, pp. 1-12. <https://doi.org/10.1016/j.susmat.2024.e00919>
- [51] Zhao, Zejia, Chujun Liu, Bo Xu, Jingwei Wang, Yingxue Yao, Tengfei Yin, Suet To, and Yang Yang. "Serrated chip formation in machining of difficult to cut metallic materials: a comprehensive review." *Critical Reviews in Solid State and Materials Sciences*, 2025, pp. 1-47. <https://doi.org/10.1080/10408436.2025.2462011>
- [52] Barik, ElunSekhar, Pankaj Charan Jena, Rajesh Kumar Behera, SunitaSethy, and SudhansuRanjan Das. "Experimental investigation and sustainability assessment in turning of newly developed AMMC (Al–Mg–Si–Cu–SiC) using coated carbide tool under minimum quantity lubrication." *Arabian Journal for Science and Engineering*, 2025, pp. 1-22. <https://doi.org/10.1007/s13369-024-09957-9>
- [53] Debnath, Kishore, Murugabalaji V, Matruprasad Rout, ManasRanjan Pal, Gorrepotu Surya Rao, and Biranchi Narayan Sahoo. "Gray relational analysis for parametric optimization of micro-EDM of thermo-mechanically processed AA7075 and AA7075/SiC/Gr composite." *Journal of Micromanufacturing*, Vol. 7, No. 2, 2024, pp. 164-180. <https://doi.org/10.1177/25165984241281024>